



Aalborg Universitet

AALBORG UNIVERSITY  
DENMARK

## Physical Modelling of Cyclic Laterally Loaded Pile in Cohesionless Soil

Hansen, Mette; Wolf, Torben K.; Rasmussen, Kristian L.; Roesen, Hanne Ravn; Ibsen, Lars Bo

*Publication date:*  
2013

*Document Version*  
Publisher's PDF, also known as Version of record

[Link to publication from Aalborg University](#)

*Citation for published version (APA):*

Hansen, M., Wolf, T. K., Rasmussen, K. L., Roesen, H. R., & Ibsen, L. B. (2013). *Physical Modelling of Cyclic Laterally Loaded Pile in Cohesionless Soil*. Department of Civil Engineering, Aalborg University. DCE Technical Memorandum No. 026

### General rights

Copyright and moral rights for the publications made accessible in the public portal are retained by the authors and/or other copyright owners and it is a condition of accessing publications that users recognise and abide by the legal requirements associated with these rights.

- Users may download and print one copy of any publication from the public portal for the purpose of private study or research.
- You may not further distribute the material or use it for any profit-making activity or commercial gain
- You may freely distribute the URL identifying the publication in the public portal -

### Take down policy

If you believe that this document breaches copyright please contact us at [vbn@aub.aau.dk](mailto:vbn@aub.aau.dk) providing details, and we will remove access to the work immediately and investigate your claim.

# **Physical Modelling of Cyclic Laterally Loaded Pile in Cohesionless Soil**

**Mette Hansen  
Torben Kirk Wolf  
Kristian Lange Rasmussen  
Hanne Ravn Roesen  
Lars Bo Ibsen**

Aalborg University  
Department of Civil Engineering

**DCE Technical Memorandum No. 026**

# **Physical Modelling of Cyclic Laterally Loaded Pile in Cohesionless Soil**

by

Mette Hansen  
Torben Kirk Wolf  
Kristian Lange Rasmussen  
Hanne Ravn Roesen  
Lars Bo Ibsen

June 2013

© Aalborg University

## **Scientific Publications at the Department of Civil Engineering**

*Technical Reports* are published for timely dissemination of research results and scientific work carried out at the Department of Civil Engineering (DCE) at Aalborg University. This medium allows publication of more detailed explanations and results than typically allowed in scientific journals.

*Technical Memoranda* are produced to enable the preliminary dissemination of scientific work by the personnel of the DCE where such release is deemed to be appropriate. Documents of this kind may be incomplete or temporary versions of papers—or part of continuing work. This should be kept in mind when references are given to publications of this kind.

*Contract Reports* are produced to report scientific work carried out under contract. Publications of this kind contain confidential matter and are reserved for the sponsors and the DCE. Therefore, Contract Reports are generally not available for public circulation.

*Lecture Notes* contain material produced by the lecturers at the DCE for educational purposes. This may be scientific notes, lecture books, example problems or manuals for laboratory work, or computer programs developed at the DCE.

*Theses* are monographs or collections of papers published to report the scientific work carried out at the DCE to obtain a degree as either PhD or Doctor of Technology. The thesis is publicly available after the defence of the degree.

*Latest News* is published to enable rapid communication of information about scientific work carried out at the DCE. This includes the status of research projects, developments in the laboratories, information about collaborative work and recent research results.

Published 2013 by  
Aalborg University  
Department of Civil Engineering  
Sohngaardsholmsvej 57,  
DK-9000 Aalborg, Denmark

Printed in Aalborg at Aalborg University

ISSN 1901-7278  
DCE Technical Memorandum No. 026

## **Recent publications in the DCE Technical Memorandum Series**

# Physical Modelling of Cyclic Laterally Loaded Pile in Cohesionless Soil

*M. Hansen<sup>1</sup>, T. K. Wolf<sup>1</sup>, K. L. Rasmussen<sup>2</sup>, H. R. Roesen<sup>3</sup> and L. B. Ibsen<sup>3</sup>*

<sup>1</sup> COWI, Lyngby, Denmark

<sup>2</sup> Niras, Aalborg, Denmark

<sup>3</sup> Department of Civil Engineering, Aalborg University, Denmark

## ABSTRACT

Offshore wind turbines are placed in a rough environment, subjected to variable lateral loads, mostly from wind and waves. A long-term lateral loading may create rotation (tilt) of the pile by change in the soil-pile system which is critical in the serviceability limit state. The accumulated rotation due to long-term lateral loading is therefore a current issue of interest as today's design guidances have little knowledge in this area. The cost of large-scale testing is extensive which make small-scale testing desirable as a tool for describing the behaviour of a soil-pile system subjected to lateral load. In this paper small-scale testing of a pile subjected to cyclic, lateral loading is treated in order to investigate the effect of cyclic loading. The test pile has a diameter of 100 mm and is 600 mm high, making the slenderness ratio 6, which resembles the ratio of offshore wind turbines today. The test pile is placed in saturated dense sand. A monotonic test is conducted to define the ultimate lateral capacity. Afterwards a cyclic test is conducted to investigate the accumulation of rotation when the pile is subjected to cyclic lateral load. Force and displacement during both tests are recorded to determine the deformation of the pile. Comparing the responses of the monotonic and the cyclic test, the cyclic test shows a stiffer response. During the cyclic test, the rotation of the pile accumulates with decreasing rotation increments. However, no stabilised situation occurs. The measured data is compared to theories on degradation, agreeing that the accumulated rotation as an estimate can be expressed by both a logarithmic and exponential expression. Comparing the results from the cyclic test with results from other recent small-scale tests shows agreement in the accumulation of rotation with decreasing rotation increments with no stabilising situation.

**KEY WORDS:** small-scale; model; tests; monopiles; cyclic; long-term; sand.

## INTRODUCTION

The monopile foundation is the most commonly used foundation for wind turbines. These foundations often have a diameter of 4 - 6 m and a slenderness ratio, the ratio between the length and the diameter of the

pile, of approximately 5 as the normal embedded length is 20 - 30 m. Long-term lateral loading of piles is an area on which the recent design guidances have little knowledge. It is of current interest since the long-term loading may create rotation (tilt) of the pile by change in the soil-pile system which is critical in the serviceability limit state (SLS).

The issue is rather complex as many parameters seem to influence the behaviour of the soil-pile system. Parameters such as load characteristic, number of load cycles and their amplitudes, and soil parameters are all possible to affect this system. Theory on the subject of cyclically loaded piles in sand have among others been presented by Long and Vanneste (1994) and Lin and Liao (1999) in terms of degradation factors. These are implemented in determining deformation of the pile by means of soil density, installation method of the pile, and load ratio. The theories are simple and give an estimate on deformations based on relatively few full-scale experiments with no more than 500 load cycles. As full-scale testing is comprehensive experimental studies in small-scale testing is pursued. In the following, the more recent work in small-scale testing in sand by Peng et al. (2006), Peralta and Achmus (2010), LeBlanc et al. (2010) and Roesen et al. (2011b) is outlined.

In order to further investigate the subject of long-term lateral loading a small-scale experiment of a pile placed in saturated soil is conducted. First a monotonic loading is applied to the pile to determine the ultimate capacity. Based on the capacity, a cyclic load is chosen and the pile is subjected to one-way cyclic loading. The test results are compared with the theoretical basis for determining effects of cyclic load.

## RECENT SMALL-SCALE CYCLIC TESTING

Peng et al. (2006) subjects a pile with a diameter of 44.5 mm and a slenderness ratio of 9 to two-way loading. The load scenarios are both balanced and unbalanced. The pile is placed in dry sand with a relative density,  $D_r = 0.72$ . Based on a few tests subjected to approximately 10000 load cycles they reach the conclusion that the soil-pile system will keep deforming with increase in number of cycles. They also

observe that larger deformation is caused by unbalanced loading in comparison with balanced loading.

Peralta and Achmus (2010) investigate one-way loading of piles with a diameter of 60 mm and varying length, describing slenderness ratios from 3.2 to 8.3. The tests are conducted in dry sand with  $D_r$  from 0.4 to 0.6. Also Peralta and Achmus (2010) experience a continuous deformation after 10 000 load cycles. They fit their results to a power and a logarithmic expression and they conclude that the deformation of the rigid piles fit the power function best and the more slender piles fit the logarithmic function.

LeBlanc et al. (2010) perform both one- and two-way loading of a 80 mm wide pile with a slenderness ratio of 4.5. The sand has  $D_r$  of 0.04 and 0.38. In several of their tests the pile is loaded with 8000 to 9000 cycles, for a few tests approximately 18000 cycles are applied and one test is conducted with 65000 cycles. In agreement with Peng et al. (2006) and Peralta and Achmus (2010) they conclude that the system keeps deforming with increase in number of load cycles. They find that a power function fit their data best.

Roesen et al. (2011b) conduct a cyclic loading test of a 100 mm wide pile with a slenderness ratio of 6. The test is of one-way loading. The pile is placed in saturated sand with relative density between 0.78 to 0.87. Approximately 46 000 load cycles is applied. In contrast to the previous tests Roesen et al. (2011b) present results where the accumulation in rotation of the pile stabilises. This happens after approximately 15 000 load cycles.

## EXPERIMENTAL PROGRAMME

Before the cyclic load test a monotonic load test is carried out. A monotonic load is applied until a predetermined rotation of the pile of  $3^\circ$  is reached. The load at this rotation will be defined as the ultimate lateral capacity. The ultimate limit state (ULS) load is used to determine the cyclic load. The size of the maximum force in a load cycle is determined based on LeBlanc et al. (2010). The load characterising fatigue limit state (FLS) and the serviceability limit state (SLS) is presented by (LeBlanc et al., (2010) as 28 to 45% of the ULS, respectively. The cyclic test is carried out as a one-way long-term lateral loading. The test setup is capable of producing more than 40 000 load cycles.

### Test Setup

The test setup is developed based on the test setup by LeBlanc et al. (2010) with some geometric deviations. For cyclic lateral loading the load characteristics are defined by the ratios  $\zeta_b$  and  $\zeta_c$  (LeBlanc et al., 2010).  $\zeta_b$  describes the ratio between the maximum cyclic moment,  $M_{max}$  and the maximum static moment capacity,  $M_S$ .  $\zeta_c$  describes the ratio between maximum and minimum moment,  $M_{min}$ , of a load cycle, cf. Eq.1. A list of symbols is in the back of the article.

$$\zeta_b = \frac{M_{max}}{M_S}, \quad \zeta_c = \frac{M_{min}}{M_{max}} \quad (1)$$

The tests are conducted in a cylinder shaped, steel container which has a diameter of 2000 mm and a depth of 1200 mm, cf. Fig. 1. The bottom of the container is equipped with equally distributed pipes and 300 mm gravel, used as draining material, which is covered with a sheet of geotextile. The pipes are perforated making a drainage system to ensure a homogeneous and saturated soil. Water level is at all times kept 20 -

40 mm above the soil surface.

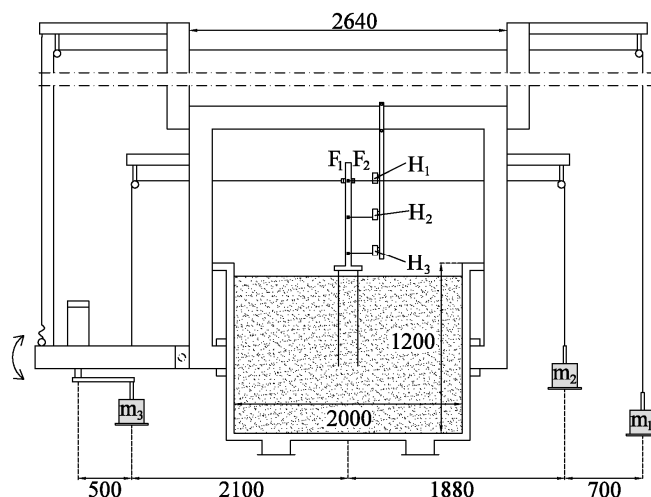


Fig. 1: Sketch of the test setup for cyclic loading with dimension in mm. F1 and F2 denote the force transducers and  $H_1$ ,  $H_2$  and  $H_3$  denote the horizontal displacement transducers.  $m_1$ ,  $m_2$  and  $m_3$  are the weights of mass.

Two different loading systems are used for the static and the cyclic load tests. The static test is conducted, by means of a motor attached to the load frame 600 mm above the soil surface, pulling the pile through a steel wire in a monotonic movement at a speed of 0.02 mm/s. The steel wire is connected to the pile via a load transducer fixated to the pile. For the static test one horizontal and two vertical displacement transducers are attached to the pile to determine the rotation of the pile, as presented by Roesen et al. (2011a). A different setup with three horizontal displacement transducers,  $H_1$ ,  $H_2$  and  $H_3$  is used for the cyclic test, cf. Fig. 1. They are placed 600 mm, 382.5 mm and 165 mm above the soil surface, respectively.

The loading system for creating cyclic load is based on the test setup by LeBlanc et al. (2010) and is a simple mechanical system of weights connected by steel wires to control the loading of the pile. A load frame with pulleys is fixated to the container connecting the masses  $m_1$ ,  $m_2$  and  $m_3$  via the wires, cf. Fig. 1. The wires also connect the masses to a lever on which a motor, providing a rotating behaviour of  $m_3$ , is attached. The lever is attached to the load frame by a pivot. Initially, the weight of  $m_1$  is chosen sufficiently to outbalance the weight of this lever, creating an outer system in balance. Masses  $m_2$  and  $m_3$  are each attached to the pile through load transducers with wires at 600 mm above the soil surface and provide the opportunity of different load scenarios as they control the cyclic load characteristic:  $m_2$  controls  $\zeta_b$  and thereby the average cyclic moment where  $m_3$  controls the cyclic amplitude, expressed by  $\zeta_c$ . The wire to the outer left is for safety, carrying no weight during the test. The motor produces a sinusoidal long-term cyclic behaviour and to simulate environmental load a rotation frequency of 0.1 Hz is used for the cyclic test (Peng et al., 2006).

The two load transducers attached through wires to  $m_2$  and  $m_3$  measure the actual load that the pile is subjected to. For static loading only one load transducer is used. All measurement equipment is connected to a PC-based data acquisition HBM Spider which transfers measuring data to the computer. Time, forces and horizontal displacements are recorded with a sampling rate of 1 Hz during long-term cyclic loading. During the static tests the sampling rate is 2 Hz.

## Procedure

The pile used in the tests is an aluminium, hollow cylinder with an outer diameter of 100 mm and a slenderness ratio of 6. The pile is installed in the middle of the container with a motor identical to that applying the load under static loading and at the same speed. For the static test a wire is mounted at 600 mm above soil surface. The pile is pulled to a rotation of 3 degrees, then unloaded completely, and reloaded to a rotation higher than 3 degrees. To out-balance the lever in the cyclic test the counterbalance  $m_1 = 27$  kg. Once the outer system is in balance the wires are mounted for the cyclic test also in a height of 600 mm above soil surface.

The maximum force during a load cycle is, preferably, 35% of the ULS load, which is the load resembling FLS. A one-way loading is desired. The combination of the weights is chosen to reach a maximum load of 35% of the ultimate capacity and a minimum load of 5 - 10 % of the ultimate capacity. To correspond the load a weight of  $m_2 = m_3 = 12$  kg is placed on the rig.

## Soil Conditions

The container is filled with 300 mm of gravel and 800 mm of sand. The tests are conducted in fully saturated soil. The sand used in the test setup is Aalborg University Sand No. 1 (Baskarp Sand No. 15). Material properties can be seen in Table 1.

Table 1 Material properties for University Sand No. 1

Specific grain density $d_s$ [g/cm <sup>3</sup> ]	Maximum void ratio $e_{max}$ [-]	Minimum void ratio $e_{min}$ [-]	50%-quantile $d_{50}$ [mm]	Uniformity coefficient $U = d_{50} / d_{100}$ [-]
2.64	0.858	0.549	0.14	1.78

Homogeneity of the soil is important for the interpretation of soil parameters and for comparison of test results. Therefore, the soil is loosened by applying an upward gradient of 0.9 and hereafter the soil is prepared for testing by vibrating it so the sand will compact. Water level will at all times be kept above the soil surface. When vibrating, the water level is approximately 100 mm above the soil surface to ensure no air enters the soil. The gravel in the bottom of the container ensures proper drainage conditions and a homogeneous in-flow.

Prior to the load tests cone penetration tests (CPT) are conducted to evaluate the state of the soil. A mini cone with a diameter of 15 mm is pushed through the sand with a velocity of 5 mm/s. The cone penetrates approximately 360 mm down into the soil. A change in piston equipment before the cyclic test made it possible to penetrate further, 400 mm. For the static and the cyclic test three CPTs are conducted for each: One in the middle of the container and one to each side in a distance of 500 mm from the middle. An additional CPT test of nine CPTs is conducted to evaluate the variations in homogeneity and the compaction of the sand. All CPTs are made in a straight line parallel to the direction of the force. From the CPTs the cone resistance is obtained, cf. Fig. 2. The CPT cone is very sensitive and a proper cone resistance is first obtained when the resistance stabilises.

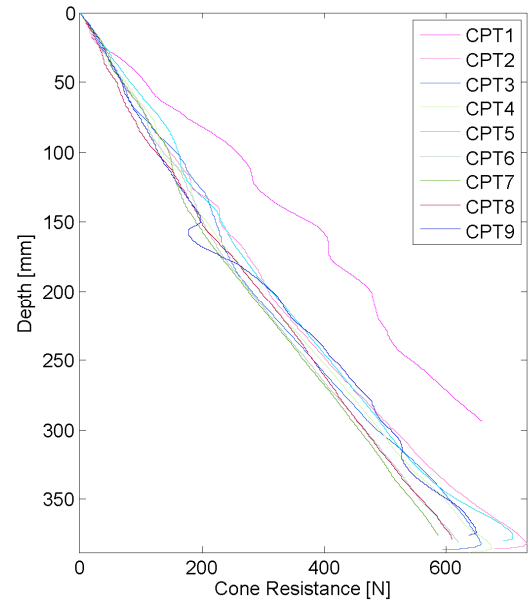


Fig. 2 Cone resistance for the nine CPTs taken additionally. The CPTs are taken in order from the passive side to the active side.

Fig. 2 shows a good resemblance among the CPTs and a smooth linear increase except for CPT 1 and CPT 9. CPT 1 shows much higher resistance and both CPT 1 and CPT 9 are more uneven in their shapes. These two CPTs are made closest to the edge of the container and are clearly affected hereby. The compaction of the sand may be different as the preparation of the sand with the vibration device is difficult along the sides. For CPT 2 to CPT 8 the soil behaves very similar and uniform and are thereby presentable data for determining soil parameters. Also, the resemblance in the cone resistance for those seven CPTs supports using three CPTs to obtain suitable data for the static test and the cyclic test.

The cone resistance is basis of further determination of soil parameters. An iterative process proposed in (Ibsen et al., 2009), Eqs. 2 to 5, is the first step in finding soil parameters.

$$\gamma = \frac{d_s + eS_w}{1 + e} \gamma_w \quad (2)$$

$$\sigma'_1 = (\gamma - \gamma_w)x \quad (3)$$

$$D_r = c_2 \left( \frac{\sigma'_1}{q_c c_1} \right)^{c_3} \quad (4)$$

$$D_r = \frac{e_{max} - e}{e_{max} - e_{min}} \quad (5)$$

where the degree of saturation,  $S_w = 1$  and  $x$  is the depth. From Eqs. 2 to 5 the unit weight,  $\gamma$ , the void ratio,  $e$ , and thereby the relative density,  $D_r$ , are derived. For both the static and the cyclic test the relative densities are shown, cf. Fig. 3.  $q_c$  is the cone resistance,  $\sigma'_1$  is the vertical effective stress and  $c_1$ ,  $c_2$  and  $c_3$  are coefficients, 0.75, 5.14 and 0.42 respectively, to determine the relative density from the mini-CPT.



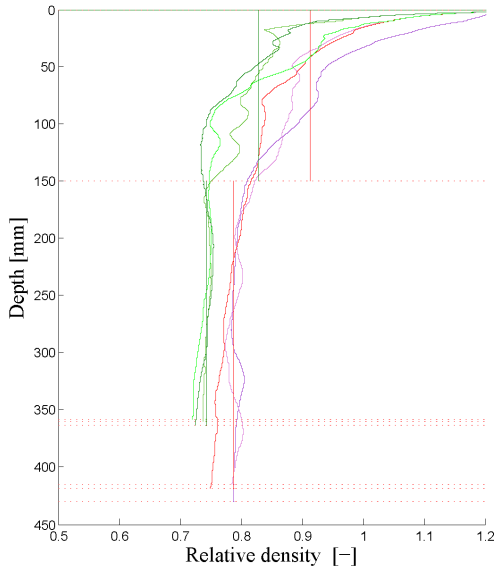


Fig. 3 The relative density of the sand for the static test and the cyclic test in green and red shades, respectively.

The three relative densities obtained from the CPTs taken before the static test are plotted in red shades and the ones made before the cyclic test are shades of green. Near the soil surface very large fluctuations are observed which is a clear sign that the CPT cone has not stabilised. Proper cone resistances are obtained after approximately 150 mm and values obtained above this depth are disregarded. A combined mean relative density for all three CPTs is made for each test. This is done separately for the relative densities above and below 150 mm under soil surface, cf. Fig. 3. This clearly illustrates that the values obtained above this limit differ from the more stabilized values below the limit. One mean value is used as representative for the entire soil layer and these are determined on behalf of values obtained from 150 mm below the soil surface and down. The mean relative density for the two tests,  $\mu$ , are given in Table 2. The standard deviations,  $\sigma$ , are also shown. It should be noted that the standard deviations are not used in any further calculations, as the parameters are not normally distributed. The values are presented for comparability only.

An interesting observation, cf. Fig. 3, is that the relative density seems to decrease slightly with depth. This behaviour is especially pronounced for the CPT made before the cyclic test. Due to overburden pressure the opposite effect would be expected. This decrease may be caused by the sand being a young deposit. Further vibration and thereby a better compaction may create an increasing relative density with soil depth.

Table 2 Mean value,  $\mu$ , and standard deviation,  $\sigma$ , of soil parameters of Aalborg University No. 1.

Test	Statistical parameter	$D_r$ [-]	$e$ [-]	$\gamma$ [kN/m <sup>3</sup> ]
Static	$\mu$	0.74	0.63	10.3
	$\sigma$	0.01	0.00	0.1
Cyclic	$\mu$	0.79	0.61	10.8
	$\sigma$	0.02	0.00	0.2

The strength parameters of the sand are calculated using formulas derived in Ibsen et al. (2009), cf. Eqs. 6 to 8. These expressions are derived for Aalborg University Sand No. 1 at confining pressures,  $\sigma'_3$ , in the range of 5 kPa to 800 kPa. As  $\sigma'_3$  is outside this range over the entire depth of the setup,  $\sigma'_3$  is set to 5 kPa in the derivation of the

strength parameters. This is considered a better estimation than using confining pressures outside the range of validity of the formulas. The results are shown in Table 3.

$$\phi_{tr} = 0.152D_r + 27.39\sigma'_3^{-0.2807} + 23.21 \quad (6)$$

$$\psi_{tr} = 0.195D_r + 14.86\sigma'_3^{-0.09764} - 9.946 \quad (7)$$

$$c = 0.032D_r + 3.52 \quad (8)$$

Table 3 Mean value,  $\mu$ , and standard deviation,  $\sigma$ , of strength parameters evaluated on basis of CPT test.

Test	Statistical parameter	$\phi$ [°]	$\psi$ [°]	$c$ [kPa]
Static	$\mu$	51.9	17.2	5.9
	$\sigma$	0.1	0.2	0.0
Cyclic	$\mu$	52.6	18.1	6.0
	$\sigma$	0.2	0.3	0.0

## TESTING RESULTS

Initially, the static test is run to determine the ultimate load capacity of the laterally loaded pile. The pile is loaded in a monotonic movement and the force-rotation relationship is shown in Fig. 4. At a force of approximately 400 N a break on the curve appears. A reason for the break may be found in the test setup. A small chain connects the wire from the motor to the pile. A slip between two links in this chain may have caused the break. The failure load is defined at a rotation of 3°. Thus, the ultimate capacity is approximate 660 N. The pile is afterwards un- and reloaded. The reloading curve continues to increase in force after having crossed the maximum force of the first load curve.

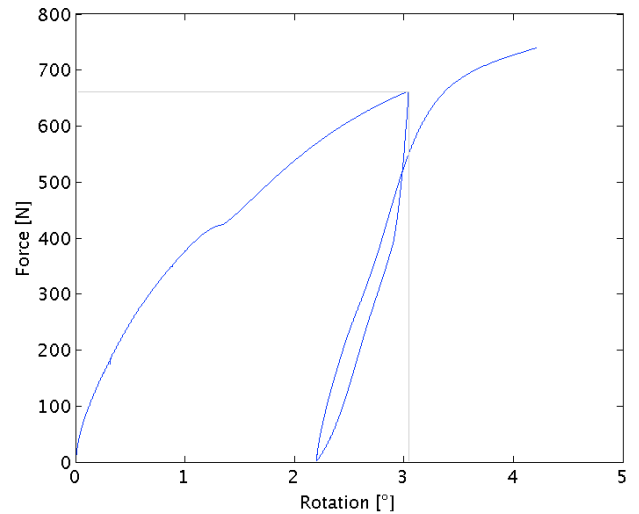


Fig. 4 The force-rotation relationship in the static test with failure determined at 3°.

The load applied as  $m_3$  for the cyclic test is determined to 12 kg. Friction in the setup can affect the system. Though, this mass is considered sufficient. Before the test is run the system is in balance. The load transducers are reset and the oscillation in load from the cyclic movement is obtained, cf. Fig. 5. The force measured from the sinusoidal loading shows similar, even load cycles for force 1,  $F1$ . A small sinusoidal behaviour is obtained from the load transducer, i.e. force 2, due to friction in the test setup or perhaps due to noise in the measurements. Force 2,  $F2$ , should remain constant during the test.

However, the variation is little and will not affect the interpretation, as the resulting force,  $F$ , affecting the pile is the difference between  $F1$  and  $F2$ , cf. Fig. 6.

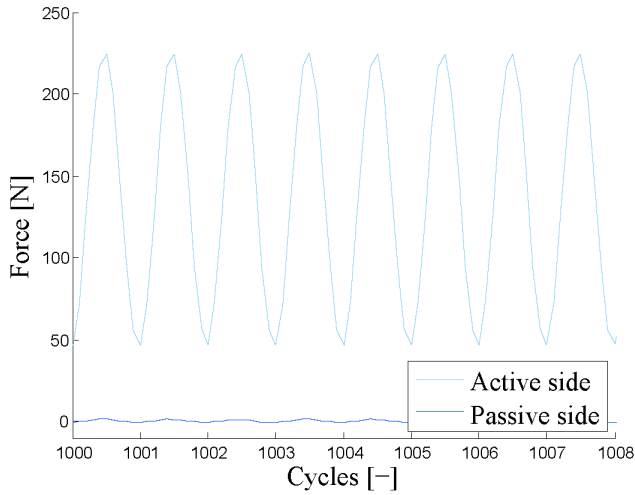


Fig. 5 Forces measured under cyclic loading. The active and passive side denote the sides of  $F1$  and  $F2$ , respectively.

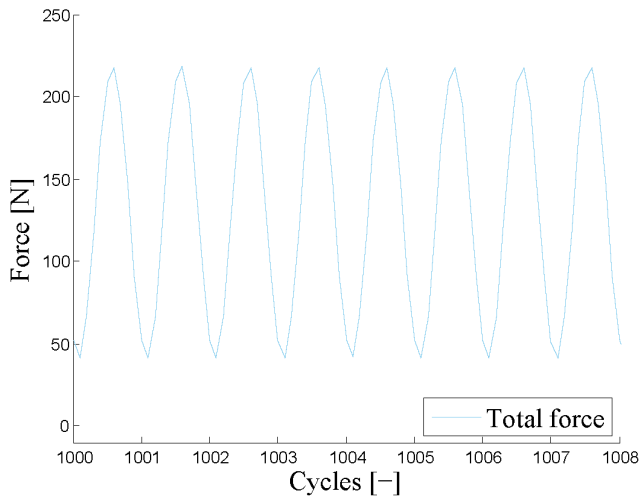


Fig. 6 Forces measured under cyclic loading.

The resulting force varies between average values of 216 N and 44 N. The force should keep a constant amplitude over time. However, the maximum force per load cycle slightly decreases over time, cf. Fig. 7. The minimum and maximum values of the minimum and maximum forces for the load cycles are given in Table 4. The difference in load may be due to friction in the setup.

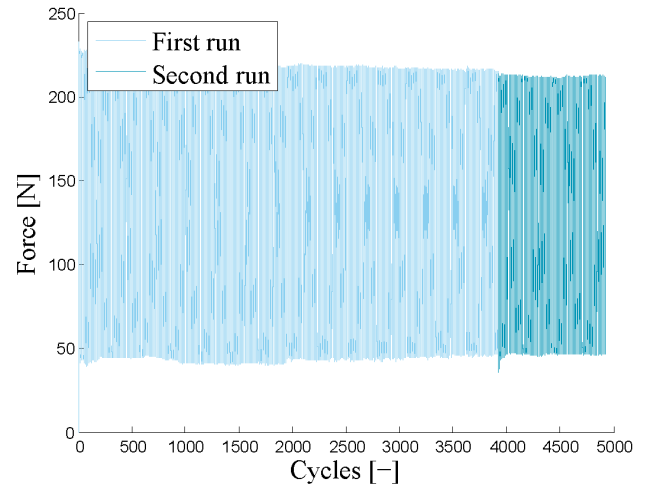


Fig. 7 Resulting force from the cyclic loading. The test stops around 3900 cycles and is started again (first and second run).

Fig. 8 shows the rotation of the pile affected by load cycles. The response is an increase in stiffness with increasing number of cycles. From the first load cycle a permanent rotation of approximately  $0.2^\circ$  is obtained and the next load cycle only creates an additional permanent rotation of less than  $0.03^\circ$ . In Fig. 8 load cycles for  $N < 2500$  are light blue and  $N > 2500$  are dark blue. The incremental accumulation in rotation decrease with number of cycles.

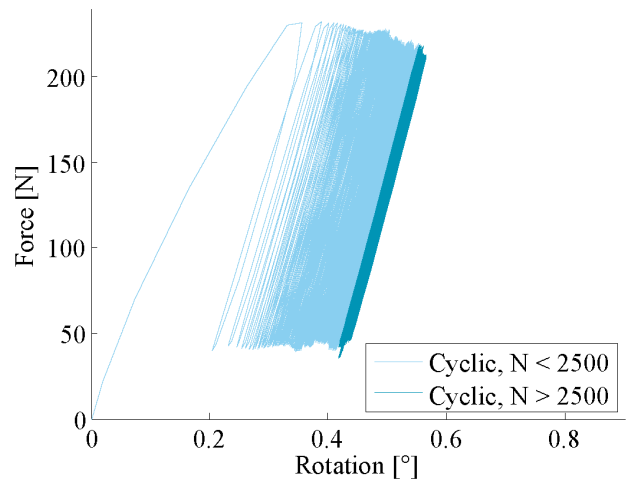


Fig. 8 Force/rotation relation at cyclic loading.

Approximately 5000 load cycles are recorded. A small increase in the load amplitude can be detected after approximately 4000 load cycles, i.e.  $0.42^\circ$  rotation, cf. Fig. 8. The cyclic test experienced a mechanical stop and was started again, which caused the irregular behaviour

The accumulated rotation after a certain number of load cycles,  $\Delta\theta(N)$ , is given for the maximum and minimum force in the load cycles. Long and Vanneste (1994) and Lin and Liao (1999) suggest that the rotation of the first load cycle is treated separately. The accumulated rotation after the first rotation is described as  $\Delta\theta(N) = \theta_N - \theta_1$ . Definitions are shown in Fig. 9.  $\theta_s$  is the rotation in a static test at the same load as the corresponding cyclic load.

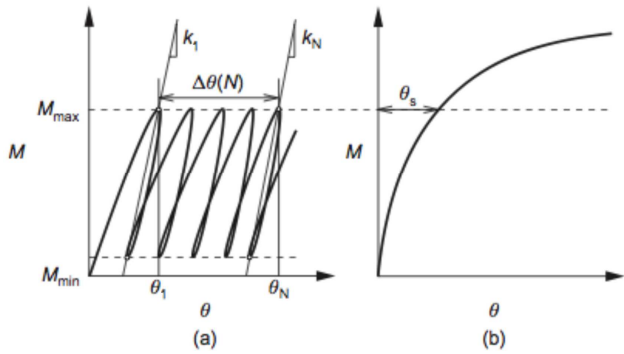


Fig. 9 The rotation as function of number of load cycles. (LeBlanc et al. 2010)

The total rotation of 100% is defined after 4919 load cycles, cf. Table 5.

Table 4 Minimum and maximum force in load cycles.

$F_{max}$ [N]	$F_{min}$ [N]
210-233	36-49

Table 5 Accumulated rotation for minimum and maximum force in the load cycles.

Load cycle $N$	$\Delta\theta(N)$ for $F_{min}$ [%]	$\Delta\theta(N)$ for $F_{max}$ [%]
10	33.4	28.6
100	66.0	64.7
1000	84.8	85.7
2000	90.3	91.6
4000	97.3	96.7
4919	100.0	100.0

The design criterion for dimensioning laterally loaded piles is related to the permanent accumulated rotation, i.e. the plastic deformations. Previous small-scale testing have determined rotation for the maximum loads, even though this rotation contain both elastic and plastic deformations. However, in agreement with Roesen et al. (2011b) it is assumed that the representative accumulated rotation for describing deformations is given by the minimum load in a load cycle. This load represents the least elastic deformation which is desirable when determining permanent rotation.

The static test and the cyclic test are plotted together in Fig. 10. The maximum cyclic force is approximately 33% of the ULS load. It appears from Fig. 10 that the cyclic test has a stiffer response than the static test. When plotting the rotation as a function of number of cycles the initial part of the curve is steep, cf. Fig. 11. The curve flattens as the accumulated rotation increments decrease. It is clear that the soil-pile system gets more stable with increase in number of load cycles. However, for the limited data a stabilised situation does not occur and increase in rotation follows with the increase in number of cycles. The rotation will keep increasing with decreasing increments.

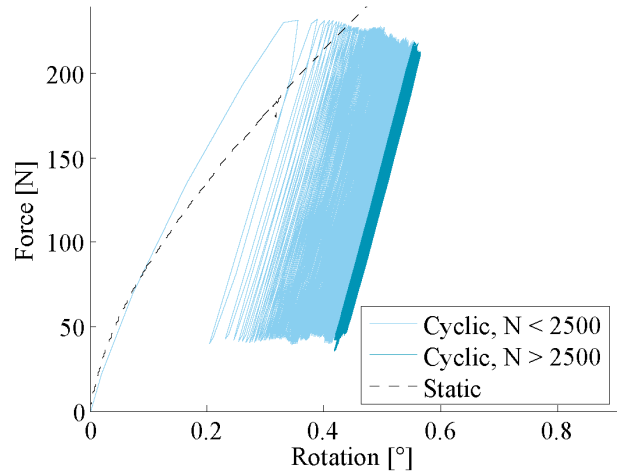


Fig. 10 The force-rotation relationship at the static test and the cyclic test.

This tendency is also experienced in other small-scale tests by Peng et al. (2006), Peralta and Achmus (2010) and LeBlanc et al. (2010), where around 10000 cycles are conducted. However, a small-scale experiment by Roesen et al. (2011b) shows stabilising behaviour. The test runs almost 46000 load cycles and after 15000 cycles no significant rotation is detected.

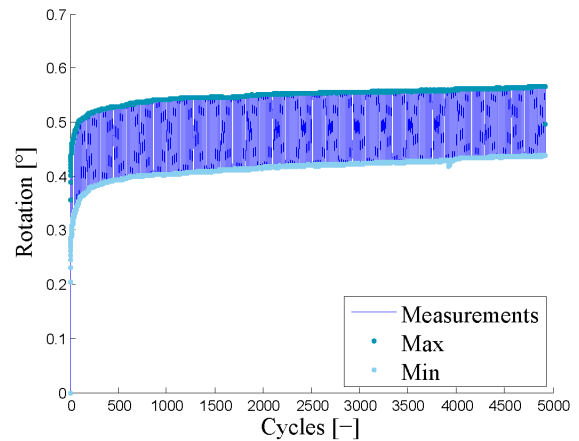


Fig. 11 The rotation as function of number of load cycles.

Two simple power and logarithmic expressions are given by Long and Vanneste (1994) and Lin and Liao (1999), respectively, Eq.9 and 10. They describe the accumulated rotation of a cyclic loaded pile and are based on tests of laterally loaded piles, cf. Hansen et al. (2012) for further clarification.

$$\frac{y_N}{y_1} = N^{\alpha m} \quad (9)$$

$$\frac{\varepsilon_N}{\varepsilon_1} = 1 + t \ln(N) \quad (10)$$

where  $m$  and  $t$  are degradation factors. The subnotation  $_N$  denotes  $N$  cycles and  $_1$  denotes the first cycle. The factor  $\alpha$  controls the relative contribution of soil resistance and deflection and is applied so change in  $p$ - $y$  relation with depth can be incorporated. The value of the factor

varies from 0 to 1. However, changing the  $\alpha$  factor provides no improvement in results, so a constant value of  $\alpha = 0.6$  is applied, making the method independent of depth.  $\varepsilon_N$  is the strain accumulation after  $N$  cycles and  $\varepsilon_1$  is the strain after the first cycle.

The two expressions are fitted by a degradation factor for a driven pile in sand with  $D_r = 0.77$  and a load characteristic corresponding to the small-scale test. These expressions are compared to the normalised maximum and minimum rotation for number of cycles, cf. Fig. 12. In Table 6 Pearson's correlation coefficient,  $R$ , and the root mean square error, RMSE, are given to describe the correlation between the measured results and the power and logarithmic function by Long and Vanneste (1994) and Lin and Liao (1999), respectively. Looking at Pearson's correlation coefficient,  $R$ , the shape of the curves for both expressions fit the data well. However, RSME, give a mean value of how close the data is fitted to the expressions. The logarithmic expression fit the minimum rotation best and the power expression fit the maximum rotation best. Since the minimum rotation is assumed to give the most exact permanent rotation the logarithmic function fits the best. However, it overestimates the rotation after the first 350 cycles. Peralta and Achmus (2010) suggest fitting accumulated rotation to power and logarithmic expressions. Also, LeBlanc et al. (2010) uses a power function.

$$\frac{\theta_N}{\theta_1} = a + b \ln(N) \quad (12)$$

where  $a$  and  $b$  are fitting coefficients and the rotation is normalised by the rotation from the first load cycle. LeBlanc et al. (2010) normalise their data differently by  $\Delta\theta(N)/\theta_s$  defined in Fig. 9. LeBlanc et al. (2010) only normalise the maximum accumulated rotations, since the minimum rotation is zero for the static rotation,  $\theta_s$ , for one-way loading with  $\zeta_c = 0$ . However, in the conducted small-scale test  $\zeta_c$  is not zero and thus the minimum rotation is normalised as well.

In Fig. 13 and Fig. 14 the logarithmic and the power functions are fitted the minimum and maximum accumulated rotation, respectively. The correlation between each function and the measured data is given by Pearson correlation coefficient,  $R$ , and RMSE in Table 7 for the minimum and maximum measured rotations. Both functions fit the measured data well with correlation coefficients between 0.959 and 0.988. The RMSE show a slightly smaller mean error for the maximum rotations. However, not one of the functions can be favoured as they are very alike. Normalising the rotation according to LeBlanc et al. (2010) makes little change. A slightly better fit is obtained by the logarithmic function according to  $R$  and RMSE. It must be emphasised that both expressions give good fits.

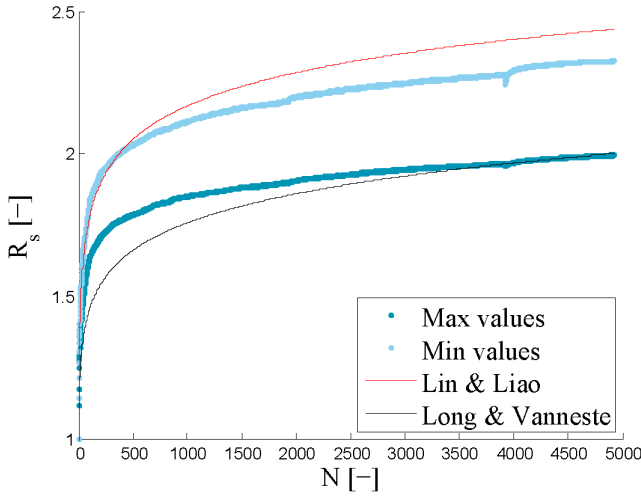


Fig. 12 The normalised maximum and minimum rotation compared to logarithmic and exponential functions by Long and Vanneste (1994) and Lin and Liao (1999).

Table 6 Pearson's correlation coefficient,  $R$ , and root mean square error between measured data and the functions by \* Long and Vanneste (1994) and \*\* Lin and Liao (1999).

		Pow.fit*	Log.fit**
$\theta(N)/\theta_1(min)$	R	0.977	0.990
	RMSE	0.339	0.090
$\theta(N)/\theta_1(max)$	R	0.973	0.989
	RMSE	0.068	0.377

The measured data is fitted the functions

$$\frac{\theta_N}{\theta_1} = aN^b \quad (11)$$

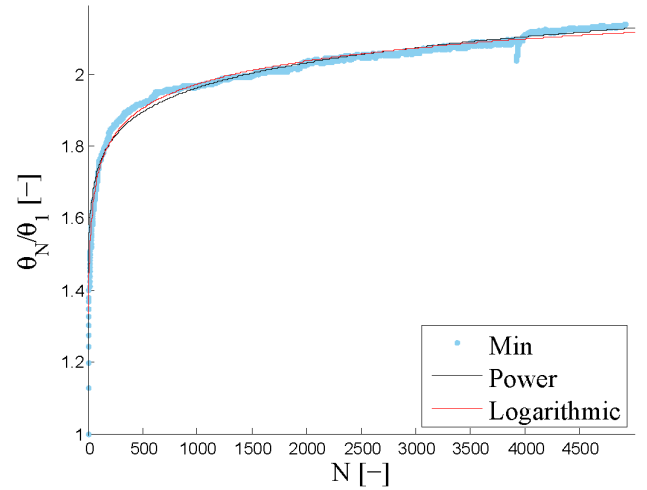


Fig. 13 Logarithmic and exponential functions fitted to minimum rotation.

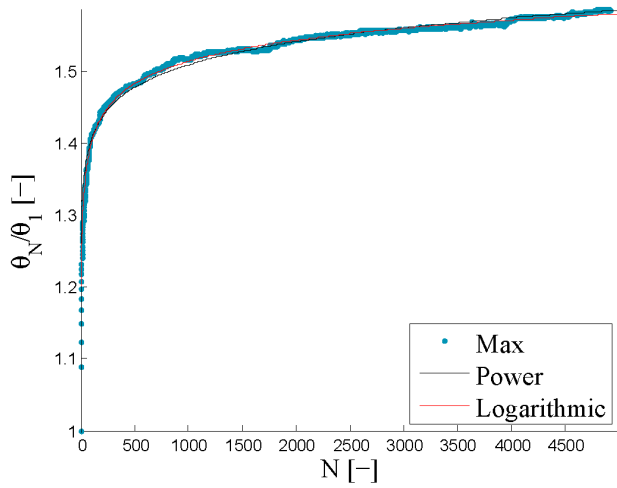


Fig. 14 Logarithmic and exponential functions fitted to maximum rotation.

Table 7 Pearsons correlation coefficient, R, and root mean square error, (RMSE), between measured data and the functions suggested by \* Peralta and Achmus (2010) and LeBlanc et al. (2010)

		Pow.fit*	Log.fit*
$\frac{\theta(N)}{\theta_1} (min)$	R	0.962	0.981
	RMSE	0.020	0.014
$\frac{\theta(N)}{\theta_1} (max)$	R	0.959	0.988
	RMSE	0.009	0.005
$\frac{\theta(N)}{\theta_s} (min)$	R	0.949	0.982
	RMSE	0.010	0.006
$\frac{\theta(N)}{\theta_s} (max)$	R	0.940	0.989
	RMSE	0.009	0.004

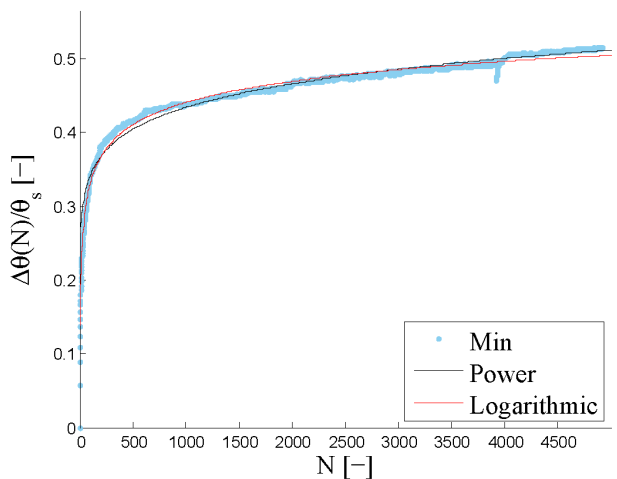


Fig. 15 Logarithmic and exponential functions fitted to minimum rotation normalised as LeBlanc et al. (2010).

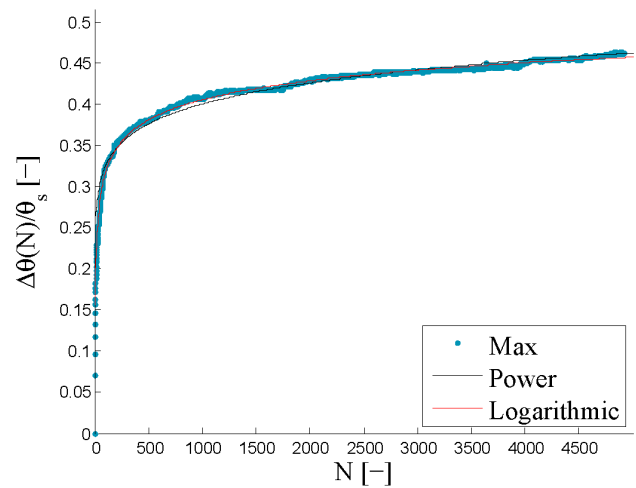


Fig. 16 Logarithmic and exponential functions fitted to maximum rotation normalised as LeBlanc et al. (2010).

## CONCLUSION

To analyse the effect that environmental forces have on offshore wind turbines small-scale testing is conducted. The test is of an aluminium pipe pile with an outer diameter of 100 mm and a length of 600 mm corresponding to a slenderness ratio of 6. The pile is placed in saturated cohesionless soil with a relative density between 74 - 79%. The relative density of the sand is determined based on CPTs conducted prior to the test. A monotonic test is conducted loading the pile to a 3° rotation and afterwards the pile is unloaded and then reloaded again. The load is applied by a motor pulling the pile with a speed of 0.02 mm/s. The ultimate capacity is defined at 3° rotation to 660 N. A cyclic load simulating FLS is chosen to approximately 35% of the ultimate capacity. This load is applied by a rotating arm with a frequency of 0.1 Hz causing a sinusoidal loading of the pile. Applied force and displacement are measured and the rotation is found.

The test results show an accumulated rotation of the pile as it is subjected to the load cycles. The rotation increments decrease with increasing number of load cycles, but no stable situation occurs. Comparing the static and cyclic test the stiffness response is larger for the cyclic test. The stiffer response may be due to different relative densities in the two tests. The frequency of which the load is applied may have an influence as the cyclic load is applied approximately 190 times faster than the cyclic load. The results give an indication of the expected behaviour of long-term loading of piles in sand. However, further investigations with a larger number of load cycles should be conducted, as 5000 cycles does not describe long-term loading.

Long and Vanneste (1994) and Lin and Liao (1999) suggest degradation of stiffness of the soil-pile system based on large-scale experiments of maximum 500 load cycles. The degradation is influenced by the relative density, the installation method and the load ratio. Lin and Liao (1999) also included a depth coefficient in the degradation. Long and Vanneste (1994) and Lin and Liao (1999) suggest a power and a logarithmic expression, respectively. Both expressions give a simple estimate of the accumulated rotation for the number of cycles applied. However, the methods are not clear on whether the rotation should be found as the maximum or the minimum rotation for a load cycles. It is the authors opinion that the minimum rotation in a load cycle represents the permanent rotation best as the elastic deformation is at its minimum as well.

Recent small-scale testing provides information on rotation of a cyclically loaded pile. Peng et al. (2006), Peralta and Achmus (2010) and LeBlanc et al. (2010) test different load scenarios with approximately 10000 cycles applied. They all agree with the measured results that rotation will keep increasing with number of load cycles. Peralta and Achmus (2010) and LeBlanc et al. (2010) suggest fitting of data by a power and logarithmic expression. The measured results can be fitted well by both expressions. Here, it should be kept in mind that the measured results only include less than 5000 cycles. Roesen et al. (2012b) measures cyclic loading of a pile subjected to approximately 46000 cycles. A stabilisation seems to occur around 15000 load cycles.

#### ACKNOWLEDGEMENT

This research is associated with the EUDP programme “Monopile cost reduction and demonstration by joint applied research” funded by the Danish energy sector. The financial support is sincerely acknowledged.

#### REFERENCES

- Rasmussen, K. L., Hansen, M., Wolf, T. K., Ibsen, L. B., Roesen, H. R. 2012 “A literature study on the effects of cyclic lateral loading of monopiles in cohesionless soil”. *DCE Technical Memorandum No. 25*, Department of Civil Engineering, Aalborg University, Denmark.
- Ibsen, L. B., Hanson, M. Hjort, T. and Taarup, M. 2009. MC-parameter Calibration of Baskarp Sand No. 15, *DCE Technical Report No. 62*. Department of Civil Engineering, Aalborg University
- LeBlanc, C., Houlsby, G. and Byrne, B. (2010). “Response of stiff piles to long-term cyclic lateral load”. *Géotechnique*, 60 (2), pp. 79-90.
- Lin, S.-S., and Liao J.C. (1999) “Permanent Strains of Piles in Sand due to Cyclic Lateral Loads”, *Journal of Geotechnical and Geoenvironmental Engineering*, 125 (9). pp. 789-802
- Long J. H. and Vanneste G. (1994) “Effects of Cyclic Lateral Loads on Piles in Sand”. *Journal of Geotechnical Engineering*, 120 (1), pp. 225-244.
- Peng, J.-R., Clarke, B. G. and Rouainia, M. (2006). “A device to Cyclic Lateral Loaded Model Piles” *Geotechnical Testing Journal* 29 (4) pp. 1-7.
- Peralta, P. and Achmus, M. (2010) “An experimental investigation of piles in sand subjected to lateral cyclic loads” *7th International Conference on Physical Modeling in Geotechnics*, Zurich, Switzerland.
- Roesen, H. R., Ibsen, L. B., and Andersen, L. V. (2012a). “Small-Scale Testing Rig for Long-Term Cyclically Loaded Monopiles in Cohesionless Soil”, *Proceedings of the 16<sup>th</sup> Nordic Geotechnical Meeting*, Copenhagen, 9-12 May, 2012, vol. 1/2, p.435-442..
- Roesen, H. R., Andersen, L. V., Ibsen, L. B. and Foglia, A. (2012b) “Experimental Setup for Cyclic Lateral Loading of Monopiles in Sand.” *Proceedings of the Twenty-second International Offshore and Polar Engineering Conference*, Rhodes, Greece.

